Construction and Building Materials 49 (2013) 635–642

Contents lists available at ScienceDirect

Construction and Building Materials

journal homepage: www.elsevier.com/locate/conbuildmat

Early-age strain–stress relationship and cracking behavior of slag cement mixtures subject to constant uniaxial restraint

Ya Wei [a,*], Will Hansen [b]

[a] Key Laboratory of Civil Engineering Safety and Durability of China, Education Ministry, Department of Civil Engineering, Tsinghua University, Beijing 100084, China
[b] Department of Civil and Environmental Engineering, University of Michigan, 2340 Hayward, Ann Arbor, MI 48109, USA

HIGHLIGHTS

- A rig was developed to measure restrained stress starting right after casting.
- Thermal and autogenous shrinkage contributions to restrained stress were recognized.
- A constitutive relationship exists between restrained shrinkage and tensile stress.
- The cracking behaviors were described for slag cement and OPC systems.

ARTICLE INFO

Article history:
Received 25 December 2012
Received in revised form 4 August 2013
Accepted 29 August 2013
Available online 25 September 2013

Keywords:
Cracking potential
Effective modulus
Restrained shrinkage
Shrinkage rate
Slag cement
Strain–stress relationship

ABSTRACT

In this study, the early-age strain–stress development of mixtures containing slag cement was measured on uniaxially restrained specimens using a specially designed testing frame starting right after casting. It was found that thermal deformation dominates early-age stress development in low w/cm and low slag cement paste systems. While for concrete, autogenous shrinkage is the major contributing factor for tensile stress development. The early-age stress development of uniaxially restrained cementitious mixture specimens is profoundly influenced by the overt early-age relaxation effect, such that the compressive stress is significantly reduced and tensile stress develops before shrinkage begins. A linear shrinkage and tensile stress relationship is found to exist in mixtures subject to such constant restraint, regardless of w/cm and slag cement contents. Slag cement has the benefit of delaying tensile stress development and cracking time because of the reduced early-age thermal effect as compared to the ordinary Portland cement mixture. The cracking of the slag cement mixture is mainly due to the greater long-term autogenous shrinkage. The cracking time is found closely related to the shrinkage rate rather than the shrinkage magnitude, a unique relationship can be used to describe such phenomenon.

1. Introduction

Concrete structures experience volume changes as a result of thermal- and moisture-related deformations during hardening. For structures subject to external restraint from surrounding substrate or internal restraint from size effect, tensile stress develops due to the restrained shrinkage, which contributes to the pre-mature cracking and affects the durability of newly constructed or repaired structures. Quantifying shrinkage induced stress and assessing the associated cracking potential in concrete members have been difficult due to many factors involved, such as stress relaxation, combined thermal and hygral effects. Several test methods have been proposed to assess cracking potential of concrete, including tests using restrained ring specimens [1–3] and tests using uniaxially restrained specimens [4–7]. The cracking potential of concrete has been classified as four categories of low, low to moderate, moderate to high, and high, based on time-to-cracking and stress rates obtained from the restrained ring test with specimens exposed to external drying conditions [8,9].

On the other hand, slag cement has been widely used in concrete structures due to many advantages, such as less carbon dioxide emission during the production process, lower hydration heat, lower permeability, and better resistance to sulphate attack [10]. However, cementitious mixtures containing slag cement have been observed to show a crossover effect with lower autogenous shrinkage at very early ages and greater autogenous shrinkage at later ages [11–13]. The tensile stress development and the associated cracking potential might be an uncertainty, as they are the coupled effect from both thermal contraction and shrinkage deformation.

The evaluation of cracking stress of structures requires material properties determined in a system subject to the similar restraint conditions to the field structures. For this purpose, this study measures strain–stress development in the uniaxially restrained

* Corresponding author. Tel.: +86 1062771646; fax: +86 1062785836.
E-mail address: yawei@tsinghua.edu.cn (Y. Wei).

0950-0618/$ - see front matter © 2013 Elsevier Ltd. All rights reserved.
http://dx.doi.org/10.1016/j.conbuildmat.2013.08.061

cement paste and concrete specimens, starting at very early ages using a specially designed rig. To investigate the pozzolanic effects, concretes containing slag cement are tested as well. A constitutive relationship between shrinkage and the restrained tensile stress was found for mixtures subject to constant uniaxial restraint. Mixtures containing slag cement show delayed time at cracking. The cracking potential depends on shrinkage rate. The results of this study are of significance for evaluating and mitigating early-age cracking in concrete members.

2. Experimental programs

2.1. Materials and mixture proportions

Type I ordinary Portland cement (OPC) and slag cement (Grade 120) were used as cementitious materials. The replacement levels of slag cement were 0%, 30% and 50% by mass of the total cementitious materials. The chemical composition and physical properties of each materials are listed in Table 1. The coarse aggregate was crushed limestone with a maximum size of 12.5 mm. The fine aggregate was natural sand with a fineness modulus of 2.56.

The mixture proportions of cement pastes and concretes used in this study are presented in Table 2. Cement paste was mixed in a pan mixer. For blended systems, the slag cement was first dry-mixed with Portland cement for several minutes to achieve a uniform distribution of the solid ingredients. Water was then added to the dry ingredients and mixed for another three minutes. The amount of high-range water-reducing admixture was used and adjusted to achieve adequate workability in low water–cementitious ratio concrete (w/cm = 0.35).

2.2. Autogenous shrinkage measurement

Linear autogenous shrinkage was measured on sealed-cured specimens, using a double-walled, water-cooled, stainless steel rig, as shown in Fig. 1. The specimen cross-section was 60 mm in height, 100 mm in width, and 1000 mm in length. External drying was prevented by sealing the specimens immediately after casting using two layers of polystyrene sheets. External restraint between the specimen and the stainless steel rig was kept to a minimum by placing a soft, flexible, 2 mm-thick foam rubber between the rig and the sealed specimen. The curing temperature was maintained at 23 ± 1 °C by circulating water through the double-walled chamber built-into the sides and bottom of the rig. One end of the specimen was fixed to the rig and the other end was free to move horizontally. The free end had an LVDT attached for measuring the autogenous deformation continuously. The measurement was initiated after final set and the data were recorded every 10 min.

2.3. Uniaxially restrained stress measurement

The restrained test measures stress development in the cementitious mixtures starting immediately after casting using a horizontal testing frame built for this purpose (shown in Fig. 2). Such a linear measuring system, according to Weiss and Shah [1], has the advantage of relatively straightforward data interpretation. The frame used in this study includes a load cell and an actuator with servo-hydraulic control. To provide sufficient restraint and to avoid drift over a long period of testing time, the actuator position was controlled, so that the concrete can be assumed to be under "full restraint" condition [14]. This type of frame is known as an active restraining rig for achieving a "full restraint" condition, which is independent of the restraining rigidity of the testing rig [14,15]. The 810 mm long specimen was cast directly into a mold held by the frame. Two ends of the specimen were enlarged and the central part has a cross-section of 100 mm by 100 mm. One end of the specimen was fixed to the load cell and the other end was connected to the actuator by restraint bars that are embedded in specimen. A thin vinyl sheet was placed between the specimen and the mold to reduce frictional resistance. Immediately after casting, the upper surface of the specimen was covered with a plastic sheet to prevent evaporation. The mold was equipped with copper pipes to circulate constant-temperature (23 ± 1 °C) water from a heating–cooling control bath. During the entire testing, the specimen was cured under sealed condition. The temperature distribution in the specimen was measured at three locations along the specimen depth. It was found that the specimens had a uniform temperature distributions at all times. The measurement started immediately after casting. Load was measured during the test and the data were recorded once per minute.

3. Results and discussions

3.1. Zero-stress temperature and zero-stress strain

For a restrained sealed-cured specimen, the development of early-age stress is a result of thermal and autogenous deformations. Fig. 3 shows the typical curves of temperature, autogenous deformation, free strain, and restrained stress developments measured on a sealed-cured concrete specimen. It can be seen that after casting the temperature of mixture increases from mixing temperature to the maximum due to the accelerated cement hydration, and then drops because of the slowdown of cement hydration. The temperature stabilizes eventually at the ambient temperature. The autogenous deformation starts with autogenous expansion followed by autogenous shrinkage, while the free strain shown in Fig. 3c is a combined effect from thermal and autogenous deformation. The starting point of free strain (ε_{01}) corresponds to the first zero-stress σ_{01} where the mixture reaches final set [16] and starts strength gain. After σ_{01}, the compressive stress starts to develop due to the restrained expansion deformation generated from the temperature rise and autogenous expansion. The temperature corresponding to the first zero-stress is the first zero-stress temperature ($T_{1st\text{-}zero\text{-}stress}$). The expansion deformation and the compressive stress grow continuously with the increase of temperature and autogenous expansion, and reach maximum at the maximum autogenous expansion. Then with the temperature drop or autogenous shrinkage development, the magnitude of expansion and the compressive stress reduces. At $T_{2nd\text{-}zero\text{-}stress}$, the restrained stress switches from compression to tension, indicating that after this point, any temperature drop or autogenous shrinkage deformation, if restrained, will generate tensile stress. It should be noted that $T_{1st\text{-}zero\text{-}stress}$ is not equal to $T_{2nd\text{-}zero\text{-}stress}$, and ε_{02} corresponding to the second zero stress is not necessary to be zero, because the high relaxation property of young concrete causes most of the compressive stress to be relaxed, and thus tensile stress might generate while mixture is still in expansion.

3.2. Free strain and uniaxially restrained stress developments

The free strain and restrained stress developments of cement paste and concrete were shown in Fig. 4. The free strain was calculated based on: $\varepsilon = (T_{1st\text{-}zero\text{-}stress} - T) \cdot \alpha + \varepsilon_a$, where, T is the temperature of restrained specimen; α is the coefficient of thermal expansion of cementitious mixture; ε_a is the autogenous deformation with positive value representing the autogenous shrinkage. The cementitious mixtures containing slag cement normally has lower coefficient of thermal expansion due to the less content of calcium hydroxide of which the coefficient of thermal expansion is high [17]. Therefore, α is taken as 18×10^{-6}/°C and 15×10^{-6}/°C for OPC pastes and slag cement pastes, respectively. For concrete the α value is taken as 10×10^{-6}/°C.

It is seen that the restrained stress develops following closely with the free strain development. Cement paste shows much faster strain and stress development as compared with those of concrete, and all paste specimens cracked within the first week. The free strain of concrete develops more slowly and at a lower magnitude, which allows more time for tensile stress to be relaxed. No cracking was observed during the testing period of 12 days for concrete.

Table 1
Chemical compositions and physical properties of cementitious materials.

Materials	SiO_2 (%)	Al_2O_3 (%)	Fe_2O_3 (%)	CaO (%)	MgO (%)	SO_3 (%)	Na_2O (%)	K_2O (%)	Blaine fineness (cm^2/g)
OPC	20.4	5.04	2.51	62.39	3.43	2.75	0.25	0.67	4290
Slag	37.49	7.77	0.43	37.99	10.69	3.21	0.28	0.46	6020

Table 2
Mixture proportions of cement paste and concrete.

Mix No.	Cement (kg/m^3)	Slag cement (kg/m^3)	Water (kg/m^3)	Coarse aggregate (kg/m^3)	Sand (kg/m^3)	HRWRA (kg/m^3)	w/cm
P35O	1500	–	525	–	–	–	0.35
P35G30	1037	444	518	–	–	–	
C35O	510	–	178	387	1100	2.1	
C35G30	357	153	178	387	1100	2.1	
P40O	1395	–	558	–	–	–	0.4
P40G30	964	413	551	–	–	–	
P40G50	685	685	548	–	–	–	
P45O	1303	–	586	–	–	–	0.45
P45G30	898	385	577	–	–	–	

HRWRA = high-range water-reducing admixture.

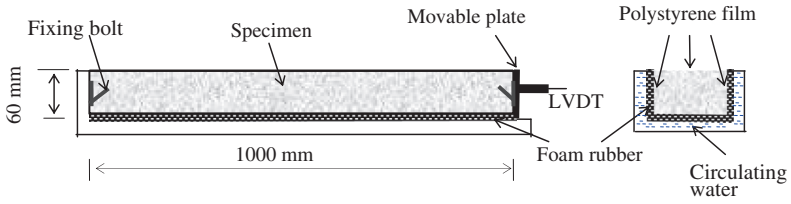

Fig. 1. Linear measurement of autogenous shrinkage of cementitious mixture.

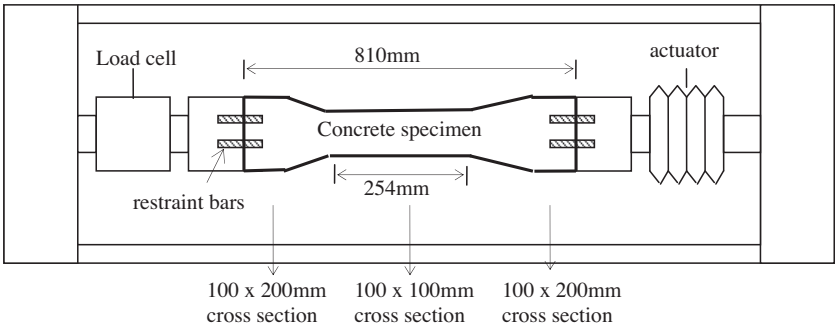

Fig. 2. Sketch of top view of the uniaxially restrained test.

The stress relaxation effect is pronounced for cementitious mixtures subject to a constant restraint condition starting at very early ages. This can be seen by comparing the free strain and the restrained stress development. All the restrained compressive stress is significantly reduced to below 0.5 MPa, though the expansion deformation can be as high as 600 microstrains. At this expansion deformation level, the instant compressive stress can reach 16.6 MPa for a hardened mixture with an elastic modulus of 27 GPa. Moreover, the high relaxation effect causes tensile stress to be generated in a mixture before shrinkage begins. As it is shown in Fig. 4, that all ε_{02} are negative. Igarashi et al. [18] also found large creep deformation in the restrained autogenous shrinkage test, and concluded that this behavior is typical for loading at very early ages.

The tensile creep behavior of concrete subject to a constant restraint is suspected to be different from that measured from conventional tensile creep test. Evaluations using existing creep models such as B3 model [19] and Østergaard model [20] proven that neither of these models produces accurate results for describing tensile creep behavior of concrete subject to constant restraint starting at very early ages [21]. The major reason might be due to the fact that these two models were developed based on conventional creep test with load applied at certain ages and no sustained restraint involved.

For a uniaxially restrained condition, another important factor that contributes to the large creep might be the "flow" property in addition to the factors such as time at loading, loading rate, and w/c ratios. Similar to plastic flow, flow in solid is found to be a consequence of stress-differences at different locations [22]. For a restrained specimen as shown in Fig. 2, the local shrinkage deformation equals at different locations, because thermal contraction and autogenous shrinkage are both independent of factors such as structure geometry and external restraint. However, there exists delay of local shrinkage stress equilibrium at different locations due to the external and internal restraints. This will cause stress-difference at different locations, and thus flow might result in such restrained concrete.

3.3. Constitutive relationship

For a restrained cementitious mixture, the tensile stress generated is normally calculated by using an integral form equation because of the continuous variation of strain levels. The equation is expressed as:

$$\sigma(t) = \int_0^t R(t,t')d[-\alpha T(t') - \varepsilon_a(t')] \quad (1)$$

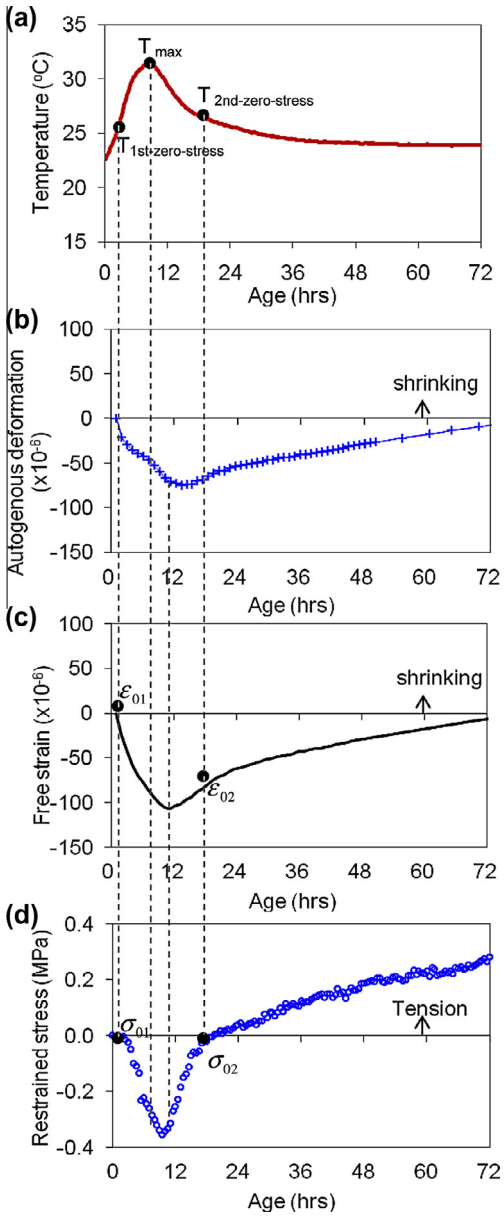

Fig. 3. Typical temperature, autogenous deformation, free strain, and restrained stress developments of a sealed-cured concrete specimen.

where $R(t, t')$ is the relaxation modulus; $T(t')$ and $\varepsilon_a(t')$ are mixture temperature and autogenous shrinkage at load application time of t'. A numerical method is generally adopted to solve Eq. (1) based on the assumption that the stress at time of t_{i+1} is the summation of the stress in the previous i time increments:

$$\sigma(t_{i+1}) = \sum_{j=1}^{i} \Delta\sigma_j(t) = \sum_{j=1}^{i} -\frac{\alpha\Delta T_j + \Delta\varepsilon_{aj}}{2}[R(t_{i+1}, t_{j-1}) + R(t_{i+1}, t_{j+1})] \quad (2)$$

where $\Delta\sigma_j(t)$ is the stress increment during time increment of j, ΔT_j and $\Delta\varepsilon_{aj}$ are the temperature change and autogenous shrinkage increment within the time increment of j.

Solving Eq. (2) appears complicated as it needs knowledge of relaxation modulus $R(t, t')$ which is difficult to obtained, especially for cementitious mixture subject to constant restraint conditions starting at very early ages, as the existing models are established based on the conventional creep test with constant load applied at ages normally later than 1 day. However, it will be desirable by conducting the following simple calculation to estimate the early-age restrained tensile stress:

$$\sigma_{tensile} = \varepsilon_s \cdot E_{eff} \quad (3)$$

where, ε_s is the shrinkage strain, E_{eff} is the effective modulus which already incorporates the creep or stress relaxation effects.

E_{eff} can be obtained from the restrained shrinkage and tensile stress curves for both paste and concrete mixtures. As shown in Fig. 5, there exists linear constitutive relationship between the restrained shrinkage strain and the tensile stress development for cementitious mixtures subject to constant restraint starting at very early ages, regardless of w/cm and slag cement content. For paste mixture, this linear relationship exists until cracking occurs. The slope of the linear curve represents the effective modulus (E_{eff}) which lumps the effects of elastic modulus, creep effect, and degree of restraint together. Low w/cm mixture shows greater slope, thus greater effective modulus. The effect of slag content on effective modulus is minor. The effective modulus for each mixtures were calculated and listed in Table 3. It can be seen that the values of effective modulus range between 2.3 GPa and 4.7 GPa, and are about 20–30% of the elastic modulus tested under compression conditions [23,24]. Paste mixtures have slightly greater effective modulus as compared to concrete. It seems that the benefit of improving concrete modulus from aggregate particles is not significant under tension loading. For this type of test, it is hypothesized in this study that the tension load is borne mostly by paste phase rather than the aggregate particle as an inclusion. The bonding between aggregate and the paste matrix is low, such that the contribution from aggregate to the effective modulus is minor, and a lower effective modulus results in concrete. For elastic modulus, however, it was measured on concrete cylinders through compressive test (ASTM C469) [25] where stiffer aggregates greatly contribute to the entire stiffness of the concrete body. This phenomenon is illustrated in Fig. 6. The effective modulus will allow engineers to easily estimate the tensile stress generated in concrete without going through the complex calculation.

3.4. Cracking behavior

As can be seen from Fig. 4 and Table 3, low w/cm pastes show earlier cracking time and higher strength at cracking. At the same w/cm, pastes containing slag cement, especially with a slag cement content of 50% by weight of the total cementitious materials, show delayed cracking time and a slightly higher cracking strength. The slag effect on delaying cracking time is pronounced in high w/cm (0.45) mixtures and in mixtures with higher slag content. As shown in Fig. 4e–h, the cracking time of P40O, P40G30, and P40G50 were 0.83 days, 1.5 days, and 5.25 days, respectively. The cracking time of P45O and P45G30 were 1.9 days and 6.08 days, respectively. There is no significant difference in cracking time of low w/cm systems (P35O vs. P35G30). The slag effect might be due to the dilution effect, that the actual Portland cement content is reduced in the blended system, leading to slower and less thermal and autogenous shrinkage deformations at early ages [13], and consequently the slower stress development. The slag effect diminishes at the lower slag cement content (30%) and in concrete mixtures. The concrete containing 30% slag cement behaved similarly to the concrete with OPC only. Therefore, it can be concluded that high slag cement content is beneficial when being used in cementitious mixture for delaying or preventing early-age cracking.

The contribution of thermal contraction and autogenous shrinkage deformation to the total shrinkage strain and consequently the tensile stress development was evaluated using the ratio of

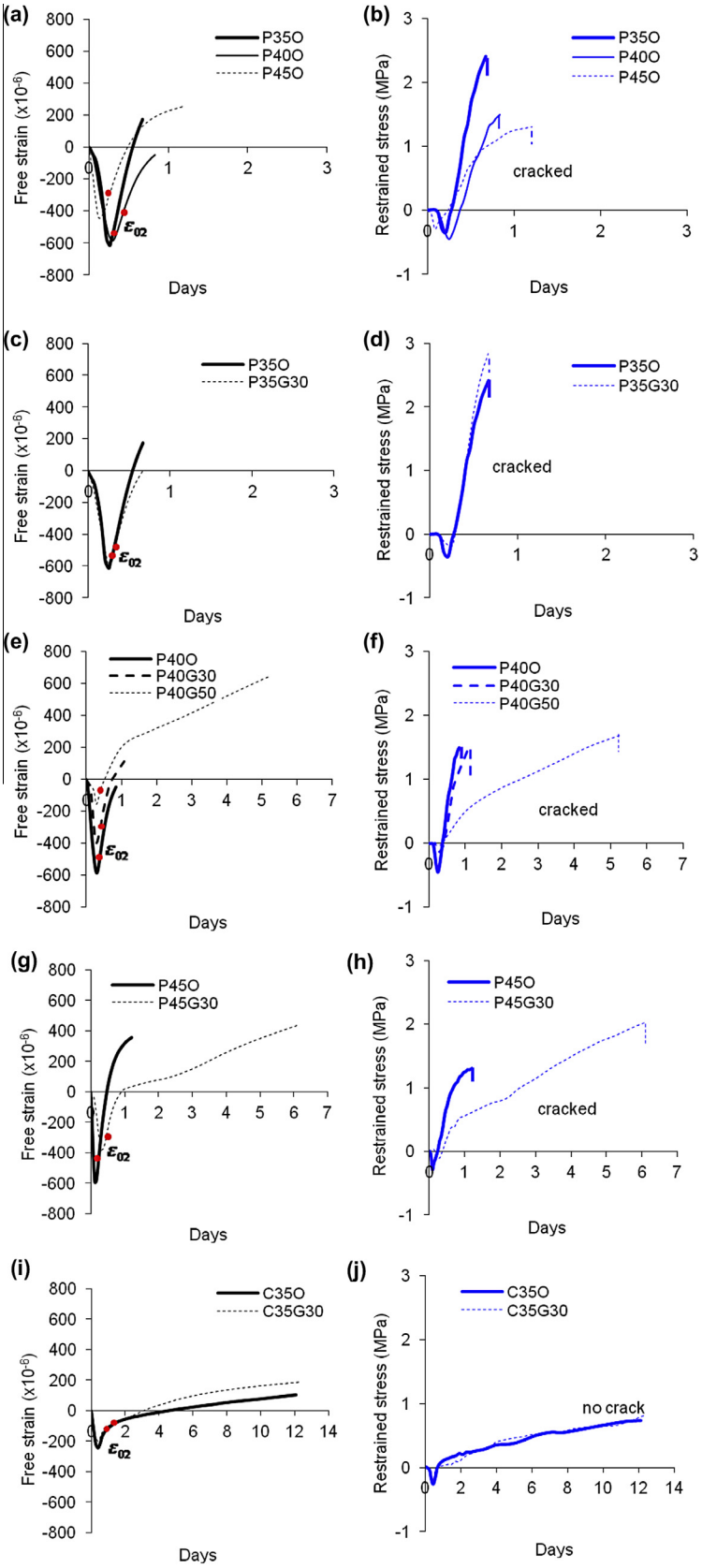

Fig. 4. Free strain and restrained stress developments in sealed-cured cement pastes and concretes.

autogenous shrinkage to the thermal contraction in this study. The autogenous shrinkage is relative to the autogenous deformation corresponding to $T_{2nd\text{-}zero\text{-}stress}$, while the thermal contraction is calculated based on $(T_{2nd\text{-}zero\text{-}stress}-T)\cdot\alpha$. As shown in Fig. 7, for OPC

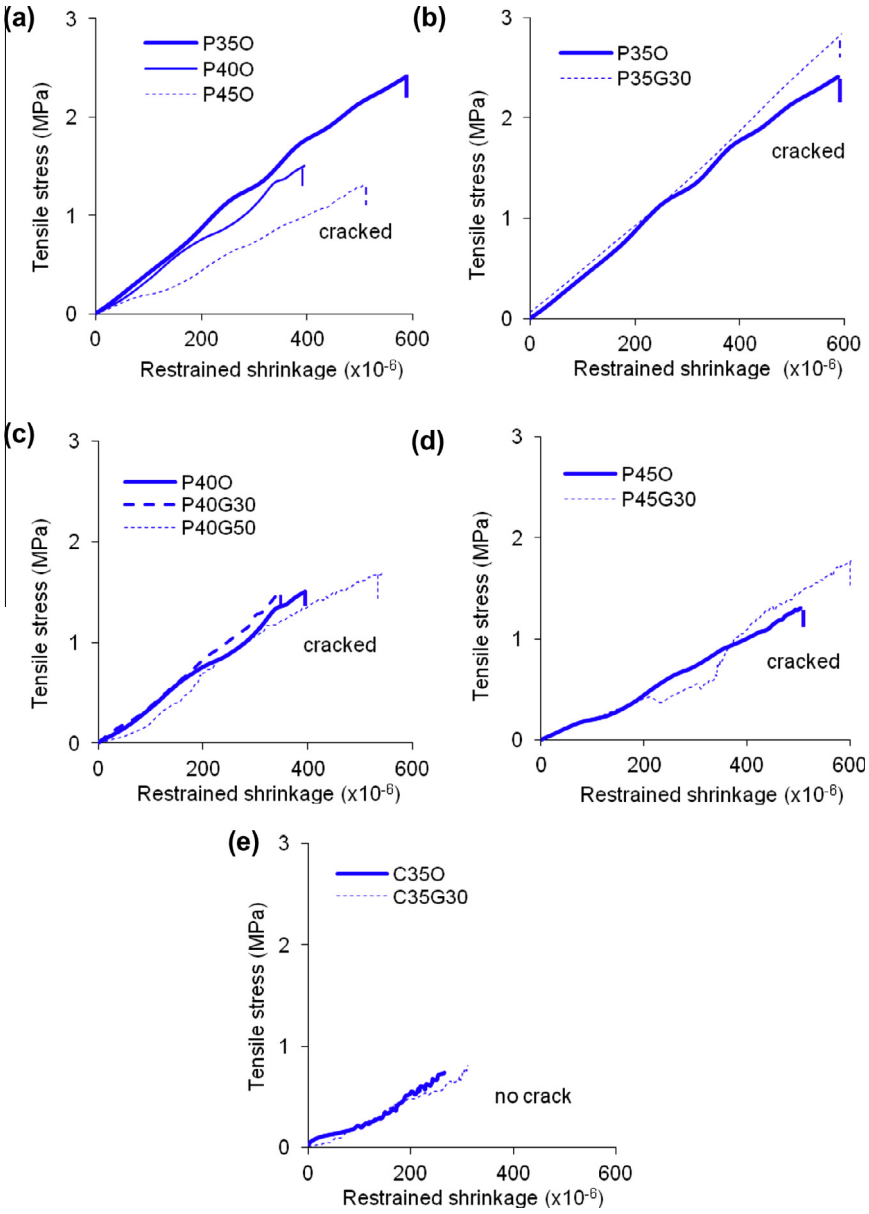

Fig. 5. Constitutive relationship between restrained shrinkage and tensile stress under constantly restrained conditions.

Table 3
Time, strength, strain rate at cracking and effective modulus of mixtures.

Mix no.	P35O	P35G30	C35O	C35G30	P40O	P40G30	P40G50	P45O	P45G30
Time at cracking (days)	0.67	0.68	–[a]	–[a]	0.83	1.5	5.25	1.9	6.08
Strength at cracking (MPa)	2.41	2.84	–[a]	–[a]	1.5	1.48	1.68	1.31	2
Strain rate at cracking ($\times 10^{-6}$/h)	42.7	34.67	–[a]	–[a]	17.34	7.13	4.27	5.3	3.36
Effective modulus (GPa)	4.2	4.7	2.3	2.3	3.8	4.2	3.3	2.5	2.8

[a] No cracking during time of testing (12 days).

paste system, the contribution from autogenous shrinkage is much less than that from thermal contraction, indicating that the tensile stress development and the cracking are mainly effects of temperature changes at early ages. For slag systems, especially in systems with high w/cm and high slag content, the contribution from the autogenous shrinkage is dominant. Because the cracking potential at early age is sensitive to the shrinkage rate rather than the magnitude of shrinkage, and the autogenous shrinkage development is more mild than that of thermal contraction in slag system with high w/cm and high slag content, and thus the cracking time was delayed in such systems. Restrained thermal contraction generally leads to the very early-age cracking at about 1 to 2 days due to the rapid temperature drop and consequently the thermal contraction.

One important observation from the above experimental results is that the development of tensile stress in a restrained specimen follows closely the shrinkage development, and a higher contraction

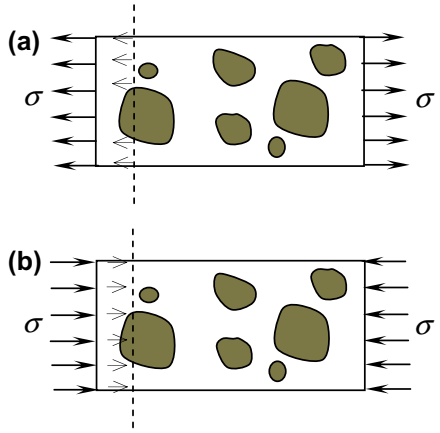

Fig. 6. Illustration of contribution of aggregate in concrete when subjected to: (a) tension and (b) compression.

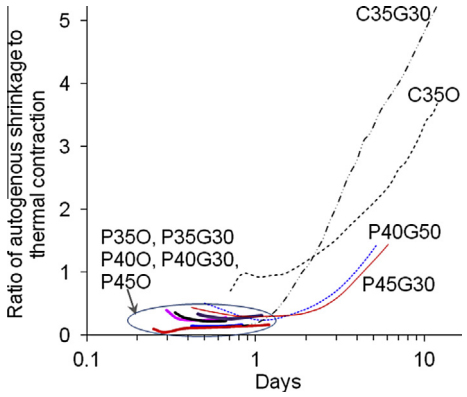

Fig. 7. Contribution of thermal contraction and autogenous shrinkage to the total shrinkage deformation.

or shrinkage rate causes earlier cracking. This observation is consistent with the previous studies [26]. Therefore, it is worthwhile to investigate the relationship between shrinkage rate ($\dot{\varepsilon}$ in microstrain/h) and the cracking time (t_{cr} in days). The shrinkage rate was calculated based on the measured shrinkage data of cement paste and concrete as $\dot{\varepsilon} = \frac{\varepsilon(t+1)-\varepsilon(t)}{\Delta t}$, in which Δt=1 h. The calculated results are shown in Fig. 8, which shows the shrinkage rate at cracking for paste specimens and the shrinkage rate of uncracked concrete specimens. It can be seen that the cracking time (t_{cr}) for paste specimens is related uniquely to the shrinkage rate at cracking or the critical shrinkage rate ($\dot{\varepsilon}_{cr}$), regardless of w/cm and the presence of slag cement. A best-fit equation can be used to describe this relationship:

$$\dot{\varepsilon}_{cr} = \left(\frac{d\varepsilon}{dt}\right)_{cr} = 14(t_{cr}/24 - 0.1)^{-0.87} \quad (4)$$

Eq. (4) is plotted in Fig. 8 and denoted as "critical shrinkage rate". It is seen that the critical shrinkage rate ($\dot{\varepsilon}_{cr}$) is related inversely to the time at cracking (t_{cr}), the smaller the critical shrinkage rate at a given time, the higher the cracking tendency of the cementitious mixture. A relationship similar to Eq. (4) but in terms of stress rate from ring test measurements has been observed previously by See et al. [26].

Since the paste phase rather than the aggregate phase is the source of shrinkage and consequently the cause of cracking in concrete, it is reasonable to assume that Eq. (4) established based on paste measurements applies to concrete mixtures as well. The shrinkage rate ($\dot{\varepsilon}$) curves of the two uncracked concrete mixtures (C35O and C35G30) are plotted in Fig. 8. These two curves are below the critical shrinkage rate curve obtained from cracked paste specimens, indicating no cracking would be expected in concrete, which is consistent with the experimental observation.

The traditional method for assessing cracking potential in cementitious mixtures requires stress measurements or calculations under restrained conditions. However, both stress measurement and calculation are difficult to conduct in field structures due to many factors involved. Establishing such a practical method for evaluating cracking potential is needed.

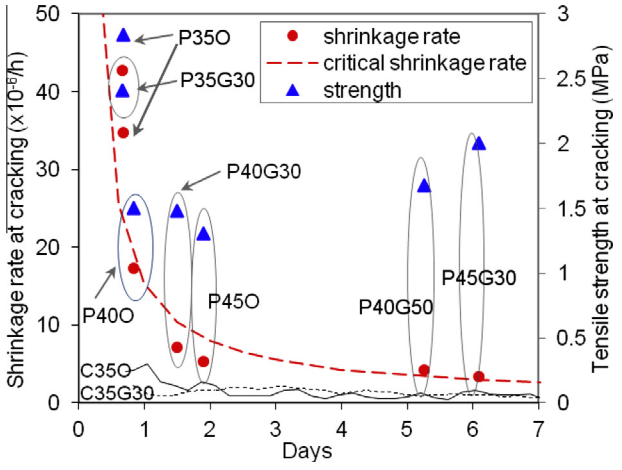

Fig. 8. Cracking behavior under uniaxially restrained conditions.

4. Conclusions

In this study, the free strain and restrained stress developments of mixtures containing slag cement were investigated on specimens subject to uniaxially restraint starting at very early ages. The major conclusions are as following:

1. A restraint rig was used to measure stress development in linear specimens starting right after casting. The induced stresses follow closely with the development of free strain. At the very early ages (1–2 days), the thermal effect dominates the developments of both compressive stress from temperature rise and tensile stress from temperature drop. Due to the very high early-age relaxation effect, the magnitude of compressive stress is greatly reduced. However, the high relaxation effect promotes tensile stress to develop while the mixtures are still in expansion.
2. Thermal deformation dominates early-age stress development in low w/cm and low slag cement paste systems. While for concrete, autogenous shrinkage is the major contributing factor for tensile stress development. All paste specimens (w/cm = 0.35, 0.4, and 0.45, with and without slag cement) cracked at ages less than 7 days because of the high shrinkage rate. Slag cement has the benefit of delaying tensile stress development and cracking time because of the reduced early-age thermal effect as compared to the ordinary Portland cement mixture. The cracking of the slag cement mixture is mainly due to the greater long-term autogenous shrinkage.
3. A linear relationship exists between the free shrinkage and the uniaxially restrained tensile stress for both cement paste and concrete, regardless of w/cm and slag cement contents. An effective modulus of mixtures under the loading and restrained conditions provided in this study was obtained to be about 20–

30% of the elastic modulus measured from instantaneous compressive test. This effective modulus incorporates the effects of both relaxation and restraint condition, and can be directly used for shrinkage stress calculation.

4. The occurrence of cracking in cementitious mixtures depends to a large extent on the shrinkage rate rather than the shrinkage magnitude. A unique relationship is found to exist between the shrinkage rate and the cracking time based on the test results on restrained linear specimens under sealed-cured conditions. The critical shrinkage rate at the time of cracking ($\dot{\varepsilon}_{cr}$) decreases rapidly within the first two days and then stabilizes.

Acknowledgement

The authors wish to thank National Science Foundation of China under Grant No. 51108246 for the supports.

References

[1] Weiss WJ, Shah SP. Recent trends to reduce shrinkage cracking in concrete pavements. In: Aircraft/pavement technology: in the midst of change, sponsors: asce, air transport division, airfield pavement committee. Seattle (WA): American Society of Civil Engineers; 1997. p. 217–28.
[2] Bentur A. Early age shrinkage induced stresses and cracking in cementitious systems. RILEM technical committee 191-EAS. RILEM Publications; 2003. 337pp.
[3] Kovler K, Sikuler J, Bentur A. Restrained shrinkage tests of fiber reinforced concrete ring specimens: effect of core thermal expansion. Mater Struct 1993;26:231–7.
[4] Springenschmid R, Gierlinger E, Kernozycki W. Thermal stress in mass concrete: a new testing method and the influence of different cements. In: Proceedings of the 15th international congress for large dams. Lausanne, Switzerland; 1985. p. 57–72.
[5] Kovler K. Testing system for determining the mechanical behavior of early-age concrete under restrained and free uniaxial shrinkage. Mater Struct 1994;27(170):324–30.
[6] Toma G, Pigeon M, Marchand J, Bissonnette B, Barcelo L. Early age restrained shrinkage: stress build up and relaxation. In: International research seminar: self-desiccation and its importance in concrete technology. Lund, Sweden; 1999. p. 61–71.
[7] Altoubat SA, Lange DA. Grip-specimen interaction in uniaxial restrained test. In: Balaguru P, Naaman A, Weiss W, editors. Concrete: material science to application—a tribute to surendra P. Shah, SP- 206. Farmington Hills (MI): American Concrete Institute; 2002. p. 189–204.
[8] Attiogbe EK, See HT, Miltenberger MA. Cracking potential of concrete under restrained shrinkage. In: Proceedings, advances in cement and concrete: volume changes, cracking, and durability, engineering conferences international. Copper Mountain, CO.; 2003. p. 191–200.
[9] See HT, Attiogbe EK, Miltenberger MA. Potential for restrained shrinkage cracking of concrete and mortar. Cem Concr Aggr 2002;26(2):123–30.
[10] Roy DM, Idorn GM. Hydration, structure, and properties of blast furnace slag cements, mortars, and concrete. ACI Mater J 1983;Nov–Dec:444–57.
[11] Chern JC, Chan YW. Deformations of concrete made with blast-furnace slag cement and ordinary portland cement. ACI Mater J 1989;86:372–82.
[12] Tazawa E, Miyazawa S, Kasai T. Chemical shrinkage and autogenous shrinkage of hydrating cement paste. Cem Concr Res 1995;25:288–92.
[13] Wei Y, Hansen W, Biernacki JJ, Schlangen E. Unified shrinkage model for concrete from autogenous shrinkage test on paste with and without GGBFS. ACI Mater J 2011;108(1):13–20.
[14] Bentur A, Kovler K. Evaluation of early age cracking characteristics in cementitious systems. Mater Struct 2003;36:183–90.
[15] Springenschmid R, Breitenbucher R, Mangold M. Development of the cracking frame and the temperature-stress testing machine. In: Springenschmid R, editor, Thermal cracking in concrete at early ages. Proc. RILEM Symp., E&FN SPON; 1994. p. 137–44.
[16] Schindler AK, McCullough BF. The importance of concrete temperature control during concrete pavement construction in hot weather conditions. J Transport Res Board 2002(1813):3–10.
[17] Shui Z, Zhang R, Chen W, Xuan D. Effect of mineral admixtures on the thermal expansion properties of hardened cement paste. Constr Build Mater 2010;24:1761–7.
[18] Igarashi1 S, Bentur A, Kovler K. Autogenous shrinkage and induced restraining stresses in high-strength concretes. Cem Concr Res 2000;30:1701–7.
[19] Bažant ZP, Baweja S. Creep and shrinkage prediction model for analysis and design of concrete structures: model B3. ACI SP-194. Farmington Hills (MI): American Concrete Institute; 2000. pp. 1–83.
[20] Østergaard L, Lange D, Altoubat SA, Stang H. Tensile basic creep of early-age concrete under constant load. Cem Concr Res 2001;31:1895–9.
[21] Wei Y, Hansen W. Tensile creep behavior of concrete subject to constant restraint at very early ages. J Mater Civ Eng 2013;25(9). doi:0.1061/(ASCE)MT.1943-5533.0000671.
[22] Reiner M. On volume or isotropic flow as exemplified in the creep of concrete. Appl Sci Res 1949;A1:475–88.
[23] Haecker C, Garboczi E, Bullard J, Bohn R, Sun Z, Shah SP, et al. Modeling the linear elastic properties of portland cement past. Cem Concr Res 2005;35:1948–60.
[24] Smilauer V, Bittnar Z. Microstructure-based micromechanical prediction of elastic properties in hydrating cement paste. Cem Concr Res 2006;36:1708–18.
[25] ASTM. Standard test method for static modulus of elasticity and poisson's ratio of concrete in compression, Standard C 469–02. West Conshohocken (PA): ASTM International; 2002.
[26] See HT, Attiogbe EK, Miltenberger MA. Shrinkage cracking characteristics of concrete using ring specimens. ACI Mater J 2003;100(3):239–45.